

# A toolbox of Equation-Free functions in Matlab/Octave for efficient system level simulation

John Maclean · J. E. Bunder ·

A. J. Roberts

April 8, 2020

**Abstract** The ‘equation-free toolbox’ empowers the computer-assisted analysis of complex, multiscale systems. Its aim is to enable you to immediately use microscopic simulators to perform macro-scale system level tasks and analysis, because micro-scale simulations are often the best available description of a system. The methodology bypasses the derivation of macroscopic evolution equations by computing the micro-scale simulator only over short bursts in time on small patches in space, with bursts and patches well-separated in time and

---

John Maclean

School of Mathematical Sciences, University of Adelaide, South Australia. <http://www.adelaide.edu.au/directory/john.maclean>

J. E. Bunder

School of Mathematical Sciences, University of Adelaide, South Australia. <mailto:judith.bunder@adelaide.edu.au>, <http://orcid.org/0000-0001-5355-2288> · A. J. Roberts

School of Mathematical Sciences, University of Adelaide, South Australia. <http://www.maths.adelaide.edu.au/anthony.roberts>, <http://orcid.org/0000-0001-8930-1552>

space respectively. We introduce the suite of coded equation-free functions in an accessible way, link to more detailed descriptions, discuss their mathematical support, and introduce a novel and efficient algorithm for Projective Integration. Some facets of toolbox development of equation-free functions are then detailed. Download the toolbox functions<sup>1</sup> and use to empower efficient and accurate simulation in a wide range of your science and engineering problems.

## Keywords

Multiscale methods · code toolbox · numerical algorithms

## Contents

1	Introduction . . . . .	2
2	Equation-free algorithms . . . . .	8
3	Using toolbox functions . . . . .	16
4	Discussion . . . . .	27

## 1 Introduction

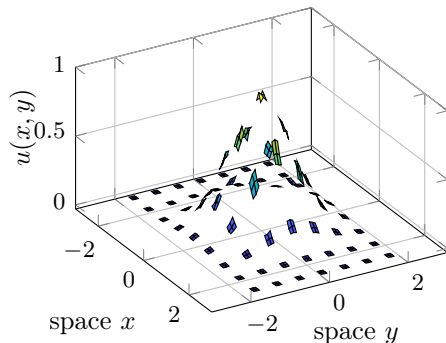
Suppose that you have a *detailed and trustworthy* computational simulation of some problem of interest. When the detailed computation is too expensive to simulate all the times of interest over all the space of interest, then the ‘Equation-Free Methodologies’ aim to accurately empower long-time simulation and system level analysis [e.g., [Kevrekidis and Samaey, 2009](#), [Kevrekidis et al.](#),

---

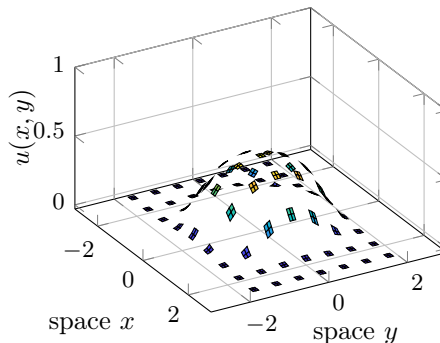
<sup>1</sup> <https://github.com/uoa1184615/EquationFreeGit>

**Figure 1** Snapshots in time of the patch scheme simulation of the nonlinear diffusive micro-scale system (1).

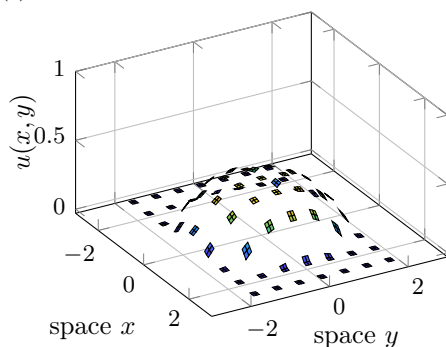
(a)  $t = 0$



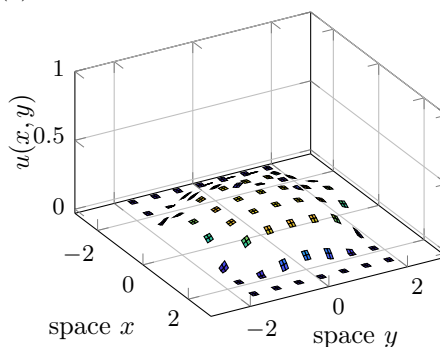
(b)  $t = 0.33$



(c)  $t = 1$



(d)  $t = 3$



2004, 2003]. Our toolbox provides you with these methodologies coded into MATLAB/Octave functions.

### 1.1 Simulation on only small patches of space

Figure 1 illustrates an ‘equation-free’ computation on only small well-separated patches of the spatial domain. The micro-scale simulations within each patch, here the nonlinear diffusive system (1), are craftily coupled to neighbouring patches and thus interact to provide accurate macro-scale predictions over the

whole spatial domain [e.g., [Roberts et al., 2014](#)]. We have proved that the patches may be tiny, and still the scheme makes accurate macro-scale predictions [[Roberts and Kevrekidis, 2007](#)]. Thus the computational savings may be enormous, especially when combined with projective integration ([Section 1.2](#)).

The example system illustrated in [Figure 1](#) is a nonlinear discrete diffusion system inspired by the lubrication flow of a thin layer of fluid, namely

$$\frac{\partial u}{\partial t} = \nabla \cdot (3u^2 \nabla u), \quad \text{equivalently} \quad \frac{\partial u}{\partial t} = \nabla^2(u^3),$$

which on a 2D micro-scale lattice  $x_{i,j}$  with tiny micro-scale spacing  $d$  is here discretised simply to

$$\frac{du_{i,j}}{dt} = \frac{u_{i+1,j}^3 + u_{i-1,j}^3 + u_{i,j+1}^3 + u_{i,j-1}^3 - 4u_{i,j}^3}{d^2}. \quad (1)$$

We want to predict the dynamics of this spatial micro-scale lattice system on the macro-scale spatial domain  $[-2, 2] \times [-3, 3]$ , but suppose full direct computation is too expensive. Instead, the micro-scale simulation illustrated by [Figure 1](#) was performed only on about 20% of the domain (it could be much less)—the small patches of space in [Figure 1](#). The key to an accurate macro-scale prediction is that each patch is coupled to nearby patches, at every computed time, by appropriate macro-scale interpolation that gives the edge values for every patch [e.g., [Roberts et al., 2014](#)].

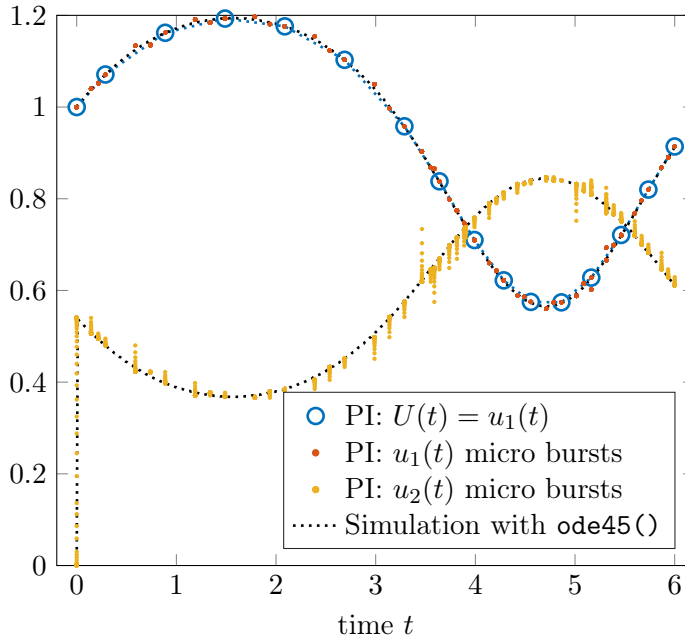
The patch scheme is most useful in applications where there is no known macro-scale closure. Then the patch scheme automatically achieves a computational macro-scale closure, without the need for any analytic construction often invoked in numerical/computational homogenization [e.g., [Saeb et al.,](#)

2016, Geers et al., 2017, Peterseim, 2019]—the patch scheme is ‘equation-free’. Our approach could be classed as a dynamic homogenization [e.g., Craster, 2015]. Frequently, problems of interest in applications compute on a micro-scale spatial lattice as in the spatial discretization (1). Suppose  $\mathbf{x}_i$  are coordinates of a micro-scale lattice, for potentially exhaustingly many lattice points indexed by  $i$ ; for example, a full atmospheric simulation. And suppose your detailed and trustworthy simulation is coded in terms of micro-field variable values  $\mathbf{u}_i(t) \in \mathbb{R}^p$  at lattice point  $\mathbf{x}_i$  at time  $t$ . When a detailed computational simulation is prohibitively expensive over all the desired spatial domain,  $\mathbf{x} \in \mathbb{X} \subset \mathbb{R}^d$ , our toolbox provides functions that empower you to use your micro-scale code as a ‘black-box’ inside only small, well-separated, patches of space by appropriately coupling across un-simulated space between the patches (Section 2.2). The toolbox functions have many options including both newly developed spectral coupling, and new symmetry preserving coupling. Section 3.2 gives an introductory tutorial.

## 1.2 Projective Integration skips through time

Simulation over time is a complementary dynamic problem. The ‘equation-free’ approach is to simulate for only short bursts of time, and then to extrapolate over un-simulated time into the future, or into the past, or perform system level analysis [e.g., Gear and Kevrekidis, 2003b, Rico-Martinez et al., 2004, Erban et al., 2006, Givon et al., 2006]. Figure 2 plots one example where the gaps in time show the un-computed times between bursts of computation.

**Figure 2** Projective Integration by the new function `PIG` of the example multiscale system (2). The macro-scale solution  $U(t)$  is represented by the blue circles ( $\circ$ ). The black dotted line, underneath the PI solution, shows an accurate micro-scale simulation over the whole time domain.



In general such a simulation is coded in terms of detailed (micro-scale) variable values  $\mathbf{u}(t)$ , in  $\mathbb{R}^p$  for some  $p$  (typically large in applications), and evolving in time  $t$ . The details  $\mathbf{u}$  could represent particles, agents, or states of a system. Both forward and backward in time computations may be performed by Projective Integration (PI) with provable accuracy [Gear and Kevrekidis, 2003b, Givon et al., 2006, Maclean and Gottwald, 2015]. For efficient simulation on long times, Section 2.1 describes how to provide your micro-scale detailed MATLAB/Octave code as a ‘black box’ to the novel Projective Integration functions in the toolbox. Section 3.1 gives a user-friendly introductory tutorial.

The example simulation of [Figure 2](#) is that of a toy system that nonetheless has challenging qualities of the multiscale phenomena that Projective Integration resolves. Here the micro-scale simulation is a pair of coupled slow-fast ODEs for  $\mathbf{u}(t) = (u_1(t), u_2(t))$ :

$$\frac{du_1}{dt} = \cos(u_1) \sin(u_2) \cos(t), \quad (2a)$$

$$\frac{du_2}{dt} = 10^5 [\cos(u_1) - u_2]. \quad (2b)$$

Using simple integration schemes, numerical solutions can be rapidly computed on micro-times of  $\mathcal{O}(10^{-5})$ , but solutions over  $\mathcal{O}(1)$  times are computationally prohibitive—except by stiff integrators. [Section 3.1.4](#) discusses scenarios where stiff integrators cannot be used or are relatively expensive, but where projective integration is effective.

The system [\(2\)](#) represents the realities of, for example, molecular dynamics simulations with rapid modes represented by  $u_2(t)$  and slow macro-scale state variables (like temperature) represented by  $u_1(t)$ . In applications the dynamics of the slow modes are usually not known, instead they emerge over the micro-scale simulation bursts [e.g., [Cisternas et al., 2004](#), [Setayeshgar et al., 2005](#), [Erban et al., 2006](#)]. Consequently, although in this toy system the slow variable  $u_1$  and fast variable  $u_2$  are obvious, here we compute only with the full system [\(2\)](#)—it is a ‘black-box’ for which we do not necessarily know what ‘variables’ are fast or slow. An alternative is to invoke algebraic analysis to construct the slow manifold of slow-fast systems like [\(2\)](#) [e.g., [Roberts, 2015](#), Ch. 4–5]: however, in many scenarios such analysis is not feasible. Since one often only measures macro-scale state variables, here we suppose the micro-

simulator only outputs  $U(t) = u_1(t)$ , called a restriction. Projective Integration (PI) uses only short bursts of the ‘black-box’ simulation, and then invokes an appropriate extrapolation to accurately predict large ‘projective’ steps. After a projective step the PI algorithm appropriately re-initialises  $u_2(t)$ , called lifting, for another burst of the micro-simulator.

Figure 2 shows the PI computation and the associated micro-scale bursts, compared to expensive simulation with `ode45()`. The micro-scale simulations with  $u_2(t)$  show the characteristic fast transients. The absolute error between the Projective Integration simulation and the trusted `ode45()` simulation is  $2 \cdot 10^{-6}$ .

The PI simulation of Figure 2 was performed by a novel function, called `PIG`, introduced in Section 2.1 and included in the toolbox. The advantage of the Projective Integration simulation over MATLAB’s `ode45()` is that PI uses only 0.6% of the number of evaluations of the ODEs (2). Section 3.1 discusses how this new PI scheme and function may be constructed through recursive use of `ode45()` which inherits all of MATLAB’s adaptive error control—an error control active on both the micro-scale and the macro-scale.

## 2 Equation-free algorithms

This section outlines the key Projective Integration and Patch Dynamics algorithms implemented in the toolbox [Roberts et al., 2020]. Pseudo-code highlights the essential features of each algorithm and the accompanying

discussion demonstrates the extended capabilities. Theoretical support for the algorithms is also discussed.

## 2.1 Algorithms for projective integration in time

Our efficient simulation of the stiff dissipative system (2) is due to the class of algorithms called Projective Integrators. Small time steps with the micro-simulator are alternated with long time steps comprised of ‘projective’ extrapolations. Sometimes PI is done with the macrostep being a Forward Euler method [Siettos et al., 2003, Chuang et al., 2015, e.g.], and so incurs global error proportional to the size of the projective time steps. Such low accuracy motivated the development of PI algorithms of provably higher accuracy [Rico-Martinez et al., 2004, Lee and Gear, 2007]. Here we additionally extend the methodology to a projective integration that invokes adaptive integrators.

The toolbox provides `PIG()`—denoting a Projective Integration with General macro-integrator and micro-simulator. The user specified macro-integrator is any integrator suitable for time stepping on the macro-scale, and includes adaptive integrators such as MATLAB’s `ode45` as used for Figure 2. Then `PIG()` provides to that integrator accurate time derivatives at the required times—time derivatives estimated from appropriate relatively short bursts of the user-defined micro-simulator `microSim()`. The effect is to do PI with any integrator, explicit or implicit, taking the projective steps. Error analyses suggested that schemes of this sort usually incur significant errors proportional to the duration of the micro-simulator burst [E, 2003, Maclean and Gottwald, 2015,

Maclean, 2015]. However, such errors are avoided by `PIG()` through a novel implementation of a ‘constraint-defined manifold computing’ scheme based on a methodology originally proposed by Gear et al. [2005], Gear and Kevrekidis [2005]. Algorithm 1 provides pseudo-code for `PIG()` that details these steps. This package is the first time such functionality for Projective Integration has been developed into a general function, tested, and made available.

Algorithm 1 outlines the essence of `PIG()`, but additional features may be invoked by a user. In particular, sometimes the projective steps are performed on a few macro-scale variables only. That is, the PI is done in a space of reduced dimension to that of the micro-simulator [Frederix et al., 2007, Bold et al., 2012, Sieber et al., 2018, e.g.]. In such cases the user provides ‘lifting’ and ‘restriction’ operators to convert between the micro- and macro-simulation spaces [Roose et al., 2009].

In addition to `PIG()`, the toolbox provides efficient integrators `PIRK2()` and `PIRK4()`, which are Projective Integrators similar to `PIG()` but with the user-defined macro-integrator replaced with second and fourth order, respectively, Runge–Kutta macro-integrators that take user specified macro-scale time-steps.

## 2.2 Algorithms to simulate on patches of space

The spatial multiscale ODEs (1) are simulated only on a fraction of space by employing a patch scheme [also known as the gap-tooth scheme, Samaey et al., 2010]. This scheme applies to dynamic systems evolving in time with some ‘spatial’ structure (‘space’ could be some other type of domain), and is useful

---

**Algorithm 1** The `PIG()` function uses short bursts of a user provided micro-scale process to simulate from time  $T_0$  to  $T$ , with initial condition  $\mathbf{u}_0$ , and via a user-specified macro-scale integrator `macroInt()`.

---

`PIG` tells the specified macro-scale integrator to use time derivatives estimated by a constraint-defined manifold function.

```

1: function PIG(macroInt(), microSim(), constrDeriv(), {T0, T}, u0)
2:   return {Tn, un}n=0^N := macroInt(constrDeriv(), {T0, T}, u0);
3: end function

```

Here, the toolbox's constraint-defined manifold function uses two applications of `microSim` and a backwards projective step in order to provide the time derivative at the time specified by `macroInt()`.

```

1: function constrDeriv(t0, u0, delta)
2:   {tm, um}m=0^M := microSim(t0, u0, delta); (burst of simulation)
3:   (du/dt)_M := (um - um-1) / (tm - tm-1); (derivative estimate at t0 + delta)
4:   v0 := um - 2*delta * (du/dt)_M; (PI backwards to t0 - delta)
5:   {sm, vm}m=0^M := microSim(t0 - delta, v0, delta); (burst of simulation)
6:   return (dv/ds)_M := (vm - vm-1) / (sm - sm-1); (derivative estimate at t0)
7: end function

```

A user provides a micro-scale simulator with the following input and output.

```

1: function microSim(t0, u0, delta)
2:   compute a burst with end time tM := t0 + delta;
3:   return {tm, um}m=0^M
4: end function

```

---

---

**Algorithm 2** Patch scheme when a user has a function  $\mathbf{fun}(t, \mathbf{u})$  that computes a time-step/time-derivative on a micro-scale lattice in space. Suppose that direct simulation is prohibitively expensive with  $\mathbf{fun}$  by some time integrator, say  $\mathbf{macroInt}(\mathbf{fun}, \{T_0, T\}, \mathbf{u}_0)$ . A user then invokes the patch scheme with the following two steps.

---

- 1: Invoke  $\mathbf{configPatches1}(\mathbf{fun}, \{a, b\}, \dots)$  to configure the patch scheme on the spatial domain  $[a, b]$  of interest (Algorithm 3).
  - 2: Then executing  $\mathbf{macroInt}(\mathbf{patchSmooth1}, \{T_0, T\}, \mathbf{u}_0)$  computes the solution on patches in space (Algorithm 4).
- 

when direct simulation over the spatial domain of interest is infeasible due to the overwhelming computational cost. The toolbox assumes that space on the micro-scale is represented as a rectangular lattice network with grid points  $\mathbf{x}_i$ —one example being the spatial discretization (1) of a PDE. The toolbox function requires the user to provide a function that computes a micro-scale time-step or time derivative for variables  $\mathbf{u}_i$  at each of the lattice nodes.

The patch scheme computes the detailed micro-scale at only a (small) subset of lattice nodes in space—the patches as illustrated by Figure 1. The scheme craftily couples the patches together to ensure macro-scale predictions are provably accurate [Roberts and Kevrekidis, 2007, Roberts et al., 2014, Bunder et al., 2017, Cao and Roberts, 2016]. For simplicity, this article discusses specifically the case of patches in 1D space, but the scheme and the toolbox extend to higher dimensional space [Roberts et al., 2014], as in the 2D simulations of Figure 1. The essence of the toolbox patch algorithms are outlined, for a specific case in 1D space, by Algorithms 2 to 4.

---

**Algorithm 3** `configPatches1` initialises the basic patch structures for [Algorithm 2](#). It creates `nPatch` equi-spaced patches inside the 1D interval  $[a, b]$ . The patches are of size proportional to `ratio` with each having `nSubP` micro-scale lattice points, and coupled by interpolation of order `ordCC`. All defined variables are saved as global for subsequent use in simulation.

---

```

1: function configPatches1(fun, {a,b}, nPatch, ratio, ordCC, nSubP)
2:    $H := (b - a)/N$ ; (distance between macro-scale mid-patches)
3:    $X_j := a + (j - \frac{1}{2})H$  for  $j := 1 : nPatch$ ; (macro-scale mid-patches)
4:    $i0 := (nSubP + 1)/2$ ; (index for the centre point of a patch)
5:    $d := (ratio \times H)/(i0 - 1)$ ; (micro-scale lattice spacing)
6:    $x_{i,j} := X_j + d(i - i0)$  for  $j := 1 : nPatch$  and  $i := 1 : nSubP$ ; (micro-scale lattice
   points in the  $j$ th patch)
7:   Calculate coefficients of interpolation to determine the edge-values of a patch
   from mid-patch values, for interpolation from ordCC/2 patches to either side of
   a patch.
8: end function

```

---

[Algorithm 2](#) introduces the necessary code for using the toolbox to implement the patch scheme on a problem of interest. In the specific case of a macro-scale 1D domain  $[a, b]$ , the toolbox function `configPatches1` ([Algorithm 3](#)) constructs `nPatch` equi-spaced patches, each of width proportional to `ratio` and each containing `nSubP` micro-scale lattice points. The integer `ordCC` determines the form and order of the inter-patch coupling that ensures macro-scale accuracy:

- even `ordCC`, the usual, and as described in [Algorithm 3](#), invokes classic Lagrange interpolation, of order `ordCC`, from mid-patch values to the

---

**Algorithm 4** Evolve in time on patches via function `patchSmooth1` which interfaces between a user’s `macroInt` and `fun`. Function `patchSmooth1` calculates the time-derivative/time-step in the interior of all patches via function `patchEdgeInt1` which couples the patches with a macro-scale interpolation.

---

```

1: function patchSmooth1( $t, u$ )
2:    $u := \text{patchEdgeInt1}(u)$ ;
3:    $\text{dudt}_{\text{interior}} := \text{fun}(t, u, x)$ ; (evaluate time-step inside every patch)
4:    $\text{dudt}_{\text{edges}, j} := 0$  for  $j := 1 : \text{nPatch}$ ;
5:    $\text{dudt} := \text{reshape}(\text{dudt}, \text{nSubP} \times \text{nPatch}, 1)$ ; (make column vector)
6:   return dudt
7: end function

1: function patchEdgeInt1( $u$ )
2:    $u := \text{reshape}(u, \text{nSubP}, \text{nPatch})$ ; (reshape so each column is a patch)
3:    $u_{\text{edges}, j} :=$  Lagrange interpolation of mid-patch values  $u_{i_0, j}$  from
    $\text{ordCC}/2$  patches to either side of each patch.
4:   return  $u$ 
5: end function

```

---

patch edge-values to generally give a macro-scale that is consistent to errors  $\mathcal{O}(H^{\text{ordCC}})$  [Roberts and Kevrekidis, 2007];

- the special case of  $\text{ordCC} = 0$ , as used in 2D for the example of Figure 1, invokes a new spectral interpolation that recent numerical experiments indicate has consistency errors exponentially small in  $H$ ;
- odd  $\text{ordCC}$  creates a scheme with a staggered grid of patches suitable for many wave systems [Cao and Roberts, 2013], staggered in the sense that mid-patch values for odd/even patches use order  $\text{ordCC}$  interpolation to determine edge-patch values of even/odd patches, respectively, and that

typically has macro-scales consistent to errors  $\mathcal{O}(H^{\text{ordCC}+1})$  [Cao and Roberts, 2016];

- and the special case of `ordCC = -1` invokes a new staggered spectral interpolation that recent numerical experiments indicate has consistency errors exponentially small in  $H$ .

After constructing the patches, a user-specified integrator `macroInt` (step 2 of Algorithm 2) simulates the user-defined `fun` over the time interval  $[T_0, T]$  with initial condition  $\mathbf{u}_0$ . Algorithm 4 overviews the toolbox function `patchSmooth1` which interfaces between the patch coupling and the user’s function `fun` that computes the micro-scale time-derivative/time-step within all the patches.

The toolbox currently implements corresponding functionality for problems in 2D space, as Figure 1 shows, via toolbox functions `configPatches2`, `patchSmooth2`, and `patchEdgeInt2`.

This patch scheme is an example of so-called *computational homogenization* [e.g., Geers et al., 2010, Saeb et al., 2016, Geers et al., 2017] and is related to *numerical homogenization* [e.g., Craster, 2015, Owhadi, 2015, Peterseim, 2019, Maier and Peterseim, 2019]. The three main distinguishing features of the patch scheme are: that a user need not perform any analysis of the micro-scale structures; that computations are done only on a (small) subset of the spatial domain; and for a wide class of systems the scheme is proved to be accurate to a user specified order [Roberts and Kevrekidis, 2007, Roberts et al., 2014, Cao and Roberts, 2016]. However, in application to micro-scale heterogeneous media—the main interest of computational/numerical homogenization—more research

needs to be done. Bunder et al. [2017] started exploring the patch scheme in heterogeneous media and established it generally has small macro-scale errors for diffusion in random media. Further, they found, analogous to that found in some numerical homogenization [Peterseim, 2019], that when the patch half-width is an integral number of periods of the micro-scale heterogeneity, then the macro-scale predictions are accurate to errors  $\mathcal{O}(H^{\text{ordCC}})$ , as before.

A recent innovation in the toolbox (by setting parameter `patches.EdgeInt=1`) is the capability to couple patches by interpolating next-to-edge values to the edge-patch values, but to the opposite edge. This coupling is the subject of an article currently in preparation which will discuss how the coupling usefully preserves symmetry in many applications of interest, and is of controllable macro-scale accuracy for micro-scale heterogeneous media.

### 3 Using toolbox functions

Users need to download the toolbox via GitHub<sup>2</sup>. Place the folder of this toolbox in a path searched by your MATLAB/Octave. The toolbox provides both a user's and a developer's manual: start by looking at the User's Manual.

Many of the main toolbox functions, when invoked without any arguments, will simulate an example. Executing the command `PIG()` reproduces the Projective Integration example presented in Section 1.2. Similarly, the nonlinear diffusion/lubrication-like example of Section 1.1 is reproduced by executing

---

<sup>2</sup> <https://github.com/uoa1184615/EquationFreeGit>

`configPatches2()`. The following [Sections 3.1](#) and [3.2](#) explain the code for both of these introductory examples as templates to adapt for other problems.

### 3.1 Invoking Projective Integration in General

This subsection discusses some key factors when constructing a Projective Integration (PI) simulation.

#### 3.1.1 Burst must be long enough, and macro-time-steps short enough

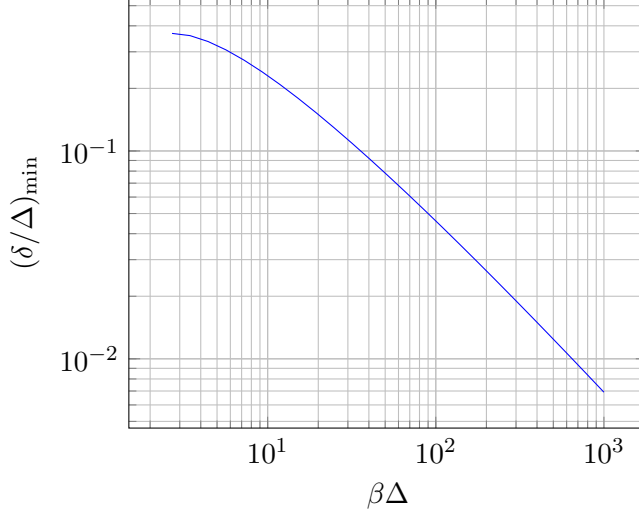
Suppose the slow dynamics of your system occurs at rate/frequency of magnitude about  $\alpha$ ; and the rate of *decay* of your fast modes are higher than the lower bound  $\beta$  (e.g., if three fast modes decay roughly like  $e^{-12t}$ ,  $e^{-34t}$ ,  $e^{-56t}$ , then  $\beta \approx 12$ ). The PI must be able to stably project the (damped) fast modes, and so the duration  $\delta$  of the micro-scale burst must be sufficiently long. The fast modes decay like  $e^{-\beta\delta}$  over the micro-burst, and then grow like  $\beta\Delta$  on a projective step of length  $\Delta$ . For stability, the product of these effects must be less than one; that is,  $\beta\Delta e^{-\beta\delta} \lesssim 1$ . Rearranging requires the burst length

$$\delta \gtrsim \frac{1}{\beta} \log |\beta\Delta| \quad (3)$$

[Figure 3](#) plots this lower bound as a function of  $\beta\Delta$  by writing  $\delta/\Delta \gtrsim \frac{1}{\beta\Delta} \log |\beta\Delta|$ .

Once stability of the fast modes is assured by satisfying (3), the accuracy of the macro-scale time-step must be considered. The second and fourth order PI functions `PIRK2()` and `PIRK4()` have global errors proportional to  $\Delta^2$  and  $\Delta^4$

**Figure 3** Minimum value (3) for  $\delta/\Delta$ , the ratio of burst length for the micro-simulator to the macro-time-step, in order to achieve stability in Projective Integration. The horizontal axis  $\beta\Delta$  is the product of the minimum decay rate for the fast modes and the macro-time-step.



respectively, for a projective step of length  $\Delta$ . More specifically, for a desired accuracy of  $\varepsilon$  and recalling that the slow dynamics occurs at rate/frequency of magnitude about  $\alpha$ : with PIRK2 we suggest  $\alpha\Delta \lesssim (6\varepsilon)^{1/2}$ ; whereas with PIRK4 try  $\alpha\Delta \lesssim \varepsilon^{1/4}$ . The accuracy of PIG() is controlled by adjusting whatever the accuracy parameters are provided to the user-specified macro-integrator.

### 3.1.2 PIG tutorial

We now discuss details of the simulation of the multiscale, slow-fast, ODES (2) shown in Figure 2. First we code the right-hand side function of the system (often people would phrase it in terms of the small parameter  $\varepsilon = 1/\beta$ ),

```
beta = 1e5;
dxdt=@(t,x) [ cos(x(1))*sin(x(2))*cos(t)
              beta*( cos(x(1))-x(2) ) ];
```

Second, we code micro-scale bursts, here using the standard `ode45()`. We choose a burst length  $(2/\beta) \log \beta$  as the fast rate of decay is approximately  $\beta$ . Because we do not know the macro-scale time-step invoked by the adaptive function to be specified for `macroInt()`, so we blithely assume  $\Delta \lesssim 1$  and then double the formula (3) for safety.

```
bT = 2/beta*log(beta);
```

Then define the micro-scale burst from state `xb0` at time `tb0` to be an integration by the adaptive `ode45` of the coded ODEs (2), over a burst-time `bT`.

```
microBurst = @(tb0, xb0) feval('ode45',dxdt,[tb0 tb0+bT],xb0);
```

Third, code functions to convert between macro-scale state  $u_1$  and micro-scale state  $(u_1, u_2)$ .

```
restrict = @(x) x(1);
lift = @(X,xApprox) [X; xApprox(2)];
```

The (optional) `restrict()` and `lift()` functions are detailed in the following [Section 3.1.3](#). Fourth, invoke PIG to use MATLAB's `ode45` on the macro-scale slow evolution. Integrate the micro-bursts over  $0 \leq t \leq 6$  from the initial condition  $\mathbf{x}(0) = (1, 0)$ .

```
Tspan = [0 6];
x0 = [1;0];
```

```
macroInt='ode45';
```

```
[Ts,Xs,tms,xms] = PIG(macroInt,microBurst,Tspan,x0,restrict,lift);
```

We pause this example to discuss the available outputs from `PIG()`. Between zero and five outputs may be requested from `PIG()`. Most often you would store the first two output results, via say `[Ts,Xs] = PIG(...)`.

- `T`, an  $L$ -vector of times at which `macroInt()` produced results.
- `X`, an  $L \times N$  array of the computed solution: the  $i$ th row of `X`, `X(i,:)`, is to be the macro-state vector  $\mathbf{X}(t_i)$  at time  $t_i = T(i)$ .

However, micro-scale details of the underlying Projective Integration computations may be helpful, and so `PIG()` provides some optional outputs of the micro-scale bursts, via `[Ts,Xs,tms,xms] = PIG(...)`

- `tms`, optional, is an  $\ell$ -dimensional column vector containing micro-scale times with bursts, each burst separated by `NaN`;
- `xms`, optional, is an  $\ell \times n$  array of the corresponding micro-scale states.

In some contexts it may be helpful to see directly how Projective Integration approximates a reduced slow vector field, via `[T,X,tms,xms,svf] = PIG(...)` in which

- `svf` is a struct containing the Projective Integration estimates of the slow vector field.
- `svf.T` is a  $\hat{L}$ -dimensional column vector containing all times at which the micro-scale simulation data is extrapolated to form an estimate of  $d\mathbf{x}/dt$  in `macroInt()`.

- `svf.dX` is a  $\hat{L} \times N$  array containing the estimated slow vector field.

If `macroInt()` is, for example, the forward Euler method (or the Runge–Kutta method), then  $\hat{L} = L$  (or  $\hat{L} = 4L$ ).

Returning to the example one remarkable feature of `PIG()` is revealed: this PI simulation, which as mentioned in [Section 1.2](#) uses only 0.6% as many evaluations of (2) as direct simulation with `ode45()`, is accomplished with a recursive call to `ode45()`. The standard MATLAB integrator is used to both compute the micro-scale bursts, and also compute the projective steps. All the usual machinery of adaptive time stepping and error control is used to regulate the micro-scale simulation, and also to regulate the macro-scale projective time-steps.

### *3.1.3 Optional PI inputs enable the user to choose how to convert between macro- and micro-scale states*

As described in the penultimate paragraph of [Section 2.1](#), the user may require an intricate or application-specific process to convert between micro-scale variables  $u$  and macro-scale variables  $U$ . Provide these bespoke functions to the toolbox PI functions with the optional inputs `restrict()` and `lift()`.

The user-provided function `restrict(u)` should map a micro-scale state  $u$ , at some fixed time, to a lower-dimensional macro-scale state  $U$  at the same time. The reverse effect is accomplished by the function `lift(U,uApprox)`, which takes two inputs—as lifting is often a non-unique process. The first input  $U$  is the macro-scale state at the (present) time at which a micro-scale state

is desired, and the second input `uApprox` is the last micro-scale state output from the micro-simulator. This `uApprox` is typically a micro-scale state from an earlier time, but nonetheless should be useful in initialising a consistent micro-scale state.

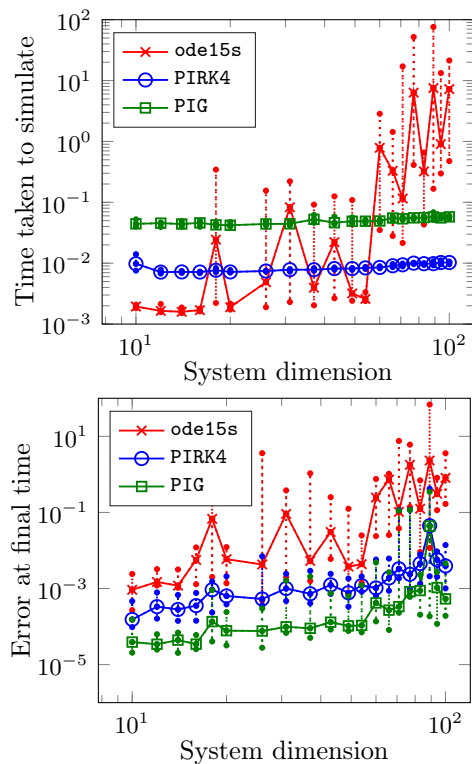
A guiding principle in the restriction and lifting functions is that we cannot anticipate a user's every need; therefore, the functions are straightforward to edit. In particular, their inputs may readily be expanded as needed.

#### *3.1.4 Choose PI over stiff integrators in high dimensions*

The 2D example of [Section 1.2](#) may be efficiently and simply simulated by standard stiff integrators, e.g. `ode15s()` in MATLAB. We here demonstrate the advantage of PI over such integrators as the model dimension increases. Consider linear systems of the form  $\frac{d\mathbf{u}}{dt} = A\mathbf{u} + \mathbf{b}$ , where  $(10 + N) \times (10 + N)$  matrix  $A$  is randomly generated so that it has ten eigenvalues with real part within  $[-0.1, 0.1]$ , corresponding to ten slow variables, and  $N$  eigenvalues with real part within  $[-20\,000, -10\,000]$ , corresponding to  $N$  fast variables. The vector  $\mathbf{b} \in \mathbb{R}^{10+N}$  is randomly generated with variance one.

We generate such a system at 20 values of  $N$  between 0 and 90, and at each one simulate to final time 10 from randomly chosen initial conditions with each of `PIRK4()`, `PIG()` and `ode15s()`. After each simulation we record the time elapsed over each simulation as well as the relative error between the simulation estimates and the exact solution. This procedure is repeated a further eleven times (the toolbox script `pirk4mance.m` details code for this

**Figure 4** Performance of Projective Integration compared to a standard stiff integrator, while scaling the dimension of the numerical model described in Section 3.1.4. Solid lines show the median, and dotted lines show the 25th and 75th percentiles. The stiff integrator is fast and reasonably accurate at low system dimension, but performs poorly at dimension 60 and above.



experiment): Figure 4 displays the recorded statistics. It appears that for system dimension larger than about 60, the cost by `ode15s` in setting up and managing the Jacobian is too high. For these larger systems, the Projective Integration functions appear the better choice.

The relative performance of `ode15s` may be improved by providing it with more information. By providing both the Jacobian  $A$  explicitly to the integrator,

and specifying the initial conditions on the attracting slow manifold, `ode15s` becomes competitive with the Projective Integration functions (up to system dimension 190). But knowing and coding both the system Jacobian and slow manifold is usually too hard in practice.

### 3.2 Patch dynamics tutorial

The code here shows one way to get started with the patch scheme. A user's script may have the following three steps (arrows indicate function recursion).

1. `configPatches2`
2. ode integrator  $\leftrightarrow$  `patchSmooth2`  $\leftrightarrow$  user's micro-scale code
3. process results

We reproduce the simulation (Figure 1) of the lattice spatial discretization (1) of a nonlinear diffusion PDE. As a micro-scale discretization of the PDE we use the following function to compute the time derivatives: an array variable `u(i,j, :, :)` refers to the  $(i, j)$ th point in each and every patch as the third and fourth indices index the 2D array of patches.

```
function ut = nonDiffPDE(t,u,x,y)

    dx = diff(x(1:2));  dy = diff(y(1:2));  % microgrid spacing

    i = 2:size(u,1)-1;  j = 2:size(u,2)-1;  % interior patch points

    ut = nan(size(u));  % preallocate storage

    ut(i,j, :, :) = diff(u(:,j, :, :).^3,2,1)/dx^2 ...
                    +diff(u(i, :, :, :).^3,2,2)/dy^2;

end
```

To use this micro-scale code on patches we need to establish global data, in struct `patches`, to characterise the patches. Here we aim to simulate the nonlinear diffusive (1) on a macro-scale  $6 \times 4$ -periodic domain with a 2D array of  $9 \times 7$  patches. Choose spectral interpolation (`ordCC = 0`) to couple the patches, and set each patch of half-size ratio 0.25 (relatively large for visualization), and with  $5 \times 5$  micro-scale lattice points within each patch. Roberts et al. [2014] established that such a patch scheme is consistent with the discretisation (1), as the patch spacing  $H$  decreases, and hence is consistent to the original PDE.

```
global patches
```

```
nSubP = 5;
```

```
configPatches2(@nonDiffPDE, [-3 3 -2 2], nan, [9 7], 0, 0.25, nSubP);
```

The third argument to `configPatches2()` is intended for boundary conditions on the macro-scale simulation, not yet implemented in the toolbox. The inputs are otherwise 2D analogues of the inputs to `configPatches1` in Algorithm 2.

For an initial condition of the simulation, here set a perturbed-Gaussian. The `reshape` functions give the  $x$  and  $y$  lattice coordinates as two 4D arrays of size  $5 \times 1 \times 9 \times 1$  and  $1 \times 5 \times 1 \times 7$  respectively. Then auto-replication fills `u0` with values from the Gaussian  $u = e^{-x^2 - y^2}$ .

```
x = reshape(patches.x, nSubP, 1, [], 1);
```

```
y = reshape(patches.y, 1, nSubP, 1, []);
```

```
u0 = exp(-x.^2 - y.^2);
```

```
u0 = u0.*(0.9 + 0.1*rand(size(u0)));
```

Initiate a plot of the simulation using only the micro-scale values interior to the patches: set  $x$  and  $y$ -edges to `nan` to leave, in plots, gaps between patches.

```
figure(1), clf
x = patches.x; y = patches.y;
x([1 end],:) = nan; y([1 end],:) = nan;
```

Start by showing the initial conditions—the top-left panel of [Figure 1](#).

```
u = reshape(permute(u0,[1 3 2 4]), [numel(x) numel(y)]);
hsurf = surf(x(:),y(:),u'); drawnow
```

Integrate in time using a standard function, or alternatively via projective integration.

```
[ts,us] = ode15s( @patchSmooth2, [0 4], u0(:));
```

Animate the computed simulation to finish with the bottom-right picture in [Figure 1](#). Use `patchEdgeInt2` to interpolate patch-edge values (even if not drawn) as it reconstitutes the row orientated output from `ode15s` into arrays that reflect the 2D patch structure.

```
for i = 1:length(ts)
    u = patchEdgeInt2(us(i,:));
    u = reshape(permute(u,[1 3 2 4]), [numel(x) numel(y)]);
    set(hsurf,'ZData', u');
    legend(['time = ' num2str(ts(i),2)])
    pause(0.1)
end
```

## 4 Discussion

This project is collectively developing a MATLAB/Octave toolbox of equation-free algorithms [Roberts et al., 2020]. The algorithms currently implement a useful functionality, but much more is desirable so the plan is to subsequently develop more capability. MATLAB/Octave appears a good choice for a first version since it is widespread, efficient, supports various parallel modes, and development costs are reasonably low. Further, it is built on BLAS and LAPACK so the cache and superscalar CPU are potentially well utilised.

Projective Integration and Patch Scheme functions are designed to generally enable users to invoke ‘equation-free’ algorithms in a wide variety of applications. In addition to simulations analogous to those in previous sections, the toolbox may empower users in other scenarios such as the following list. In the User Manual [Roberts et al., 2020] each toolbox function and application is presented in its own section, so here we refer to sections of the User Manual by using the name of the appropriate function.

- To projectively integrate in time a multiscale, slow-fast, system of ODEs with a *simple* PI macro-integrator, you could use `PIRK2()`, or `PIRK4()` for higher-order accuracy. Perhaps adapt the Michaelis–Menten example presented in the User Manual at the beginning of `PIRK2.m`.
- One may use short forward bursts of micro-scale simulation in order to stably predict the slow dynamics *backward in time* using PI [Gear and Kevrekidis, 2003a], as in `egPIMM.m`.

- 
- The lifting and restriction functions may be utilised in more complicated applications like those others have previously addressed [e.g., [Frederix et al., 2007](#), [Roose et al., 2009](#), [Bold et al., 2012](#), [Sieber et al., 2018](#)]. The lifting function has two inputs: the macro-scale state (after a macro-scale time step); and the micro-scale state at the end of the last micro-simulation. Full details for constructing these functions are in `PIG.m`.
  - For the patch scheme in 1D adapt the code at the beginning of `configPatches1.m` for Burgers' PDE, or the staggered patches of 1D water wave equations in `waterWaveExample.m`.
  - For the patch scheme in 2D adapt the code at the beginning of `configPatches2.m` for nonlinear diffusion, or the regular patches of the 2D wave equation of `wave2D.m`.
  - The previous two examples are for systems that have *smooth* spatial structures on the micro-scale: when the micro-scale is 'rough' with a known heterogeneous period (so far only in 1D), then adapt the example of `HomogenisationExample.m`.
  - Employ an ensemble of patch dynamics simulations, averaging appropriately, by adapting the example of `ensembleAverageExample.m`.
  - Combine the projective integration and patch functions to simulate a system with both time and spatial scale separation. In this case use a PI function as the integrator for a patch scheme, as done in the second portion of `ensembleAverageExample.m`.

We encourage adaptation and further development of the toolbox algorithms, and are keen to include new collaborators in future versions of the toolbox. In particular, as well as developing multi-D functions further, corresponding 1D coded functionality, we need to code and prove capability for general macro-scale boundaries. We also plan to develop projective integration for oscillatory/stochastic systems, perhaps via Dynamic Mode Decomposition [e.g., [Kutz et al., 2016, 2018](#)].

*Acknowledgements* This project is supported by the Australian Research Council via grants DP150102385 and DP180100050.

## References

- Katherine A. Bold, Karthikeyan Rajendran, Balazs Rath, and Ioannis G. Kevrekidis. An equation-free approach to coarse-graining the dynamics of networks. Technical report, [<http://arxiv.org/abs/1202.5618v1>], 2012.
- J. E. Bunder, A. J. Roberts, and I. G. Kevrekidis. Good coupling for the multiscale patch scheme on systems with microscale heterogeneity. *J. Computational Physics*, 337:154–174, may 2017. doi:[10.1016/j.jcp.2017.02.004](https://doi.org/10.1016/j.jcp.2017.02.004).
- Meng Cao and A. J. Roberts. Multiscale modelling couples patches of wave-like simulations. In Scott McCue, Tim Moroney, Dann Mallet, and Judith Bunder, editors, *Proceedings of the 16th Biennial Computational Techniques and Applications Conference, CTAC-2012*, volume 54 of *ANZIAM J.*, pages C153–C170, May 2013. doi:[10.21914/anziamj.v54i0.6137](https://doi.org/10.21914/anziamj.v54i0.6137).

- Meng Cao and A. J. Roberts. Multiscale modelling couples patches of non-linear wave-like simulations. *IMA J. Applied Maths.*, 81(2):228–254, 2016. doi:[10.1093/imamat/hxv034](https://doi.org/10.1093/imamat/hxv034).
- Claire Y. Chuang, Sang M. Han, Luis A. Zepeda-Ruiz, and Talid Sinno. On coarse projective integration for atomic deposition in amorphous systems. *The Journal of Chemical Physics*, 143(13):134703, 2015. ISSN 0021-9606. doi:[10.1063/1.4931991](https://doi.org/10.1063/1.4931991). URL <https://aip.scitation.org/doi/full/10.1063/1.4931991>.
- J. Cisternas, C. W. Gear, S. Levin, and I. G. Kevrekidis. Equation-free modeling of evolving diseases: Coarse-grained computations with individual-based models. *Proc. R. Soc. Lond. A*, 460:2761–2779, October 2004. doi:[10.1098/rspa.2004.1300](https://doi.org/10.1098/rspa.2004.1300) [1471-2946](https://doi.org/10.1098/rspa.2004.1300).
- Richard V. Craster. *Dynamic Homogenization*, volume 116 of *Springer Proceedings in Mathematics and Statistics*, pages 41–50. Springer, 2015. doi:[10.1007/978-3-319-12148-2\\_3](https://doi.org/10.1007/978-3-319-12148-2_3).
- Weinan E. Analysis of the heterogeneous multiscale method for ordinary differential equations. *Communications in Mathematical Sciences*, 1(3):423–436, 2003. doi:[10.4310/CMS.2003.v1.n3.a3](https://doi.org/10.4310/CMS.2003.v1.n3.a3).
- Radek Erban, Ioannis G. Kevrekidis, and Hans G. Othmer. An equation-free computational approach for extracting population-level behavior from individual-based models of biological dispersal. *Physica D: Nonlinear Phenomena*, 215(1):1–24, 2006. ISSN 0167-2789. doi:[10.1016/j.physd.2006.01.008](https://doi.org/10.1016/j.physd.2006.01.008). URL [http:](http://www.elsevier.com/locate/physd)

[//www.sciencedirect.com/science/article/B6TVK-4JDVNSP-1/2/f31e03e0a32cfc2a811f41ed6a8dfc6](https://www.sciencedirect.com/science/article/B6TVK-4JDVNSP-1/2/f31e03e0a32cfc2a811f41ed6a8dfc6).

- Yves Frederix, Giovanni Samaey, Christophe Vandekerckhove, and Dirk Roose. Equation-free methods for molecular dynamics: a lifting procedure. *Proc. Appl. Meth. Mech.*, 7:20100003–20100004, 2007. doi:[10.1002/pamm.200700025](https://doi.org/10.1002/pamm.200700025).
- C. W. Gear and I. G. Kevrekidis. Computing in the past with forward integration. *Phys. Lett. A*, 321:335–343, 2003a. doi:[10.1016/j.physleta.2003.12.041](https://doi.org/10.1016/j.physleta.2003.12.041).
- C. W. Gear and Ioannis G. Kevrekidis. Projective methods for stiff differential equations: Problems with gaps in their eigenvalue spectrum. *SIAM Journal on Scientific Computing*, 24(4):1091–1106, 2003b. doi:[10.1137/S1064827501388157](https://doi.org/10.1137/S1064827501388157). URL <http://link.aip.org/link/?SCE/24/1091/1>.
- C. W. Gear, T. J. Kaper, I. G. Kevrekidis, and A. Zagaris. Projecting to a slow manifold: singularly perturbed systems and legacy codes. *SIAM J. Applied Dynamical Systems*, 4(3):711–732, 2005. doi:[10.1137/040608295](https://doi.org/10.1137/040608295).
- C William Gear and Ioannis G Kevrekidis. Constraint-defined manifolds: a legacy code approach to low-dimensional computation. *Journal of Scientific Computing*, 25(1):17–28, 2005. doi:[10.1007/s10915-004-4630-x](https://doi.org/10.1007/s10915-004-4630-x).
- M. G. D. Geers, V. G. Kouznetsova, and W. A. M. Brekelmans. Multi-scale computational homogenization: Trends and challenges. *Journal of Computational and Applied Mathematics*, 234(7):2175–2182, August 2010. ISSN 0377-0427. doi:[10.1016/j.cam.2009.08.077](https://doi.org/10.1016/j.cam.2009.08.077).

- Marc G. D. Geers, Varvara G. Kouznetsova, Karel Matouš, and Julien Yvonnet. Homogenization methods and multiscale modeling: Non-linear problems. In *Encyclopedia of Computational Mechanics, Second Edition*, pages 1–34. Wiley, 2017. ISBN 978-1-119-17681-7. doi:[10.1002/9781119176817.ecm2107](https://doi.org/10.1002/9781119176817.ecm2107). URL <https://onlinelibrary.wiley.com/doi/abs/10.1002/9781119176817.ecm2107>.
- Dror Givon, Ioannis G. Kevrekidis, and Raz Kupferman. Strong convergence of projective integration schemes for singularly perturbed stochastic differential systems. *Comm. Math. Sci.*, 4(4):707–729, 2006. doi:[10.4310/CMS.2006.v4.n4.a2](https://doi.org/10.4310/CMS.2006.v4.n4.a2).
- I. G. Kevrekidis, C. W. Gear, J. M. Hyman, P. G. Kevrekidis, O. Runborg, and K. Theodoropoulos. Equation-free, coarse-grained multiscale computation: enabling microscopic simulators to perform system level tasks. *Comm. Math. Sciences*, 1:715–762, 2003. doi:[10.4310/CMS.2003.v1.n4.a5](https://doi.org/10.4310/CMS.2003.v1.n4.a5).
- I. G. Kevrekidis, C. W. Gear, and G. Hummer. Equation-free: the computer-assisted analysis of complex, multiscale systems. *A. I. Ch. E. Journal*, 50:1346–1354, 2004. doi:[10.1002/aic.10106](https://doi.org/10.1002/aic.10106).
- Ioannis G. Kevrekidis and Giovanni Samaey. Equation-free multiscale computation: Algorithms and applications. *Annu. Rev. Phys. Chem.*, 60:321–44, 2009. doi:[10.1146/annurev.physchem.59.032607.093610](https://doi.org/10.1146/annurev.physchem.59.032607.093610).
- J. Nathan Kutz, Steven L. Brunton, Bingni W. Brunton, and Joshua L. Proctor. *Dynamic Mode Decomposition: Data-driven Modeling of Complex Systems*. Number 149 in Other titles in applied mathematics. SIAM, Philadelphia,

2016. ISBN 9781611974492.

J. Nathan Kutz, J. L. Proctor, and S. L. Brunton. Applied koopman theory for partial differential equations and data-driven modeling of spatio-temporal systems. *Complexity*, (6010634):1–16, 2018. doi:[10.1155/2018/6010634](https://doi.org/10.1155/2018/6010634).

Steven L Lee and C William Gear. Second-order accurate projective integrators for multiscale problems. *Journal of Computational and Applied Mathematics*, 201(1):258–274, 2007.

John Maclean. A note on implementations of the boosting algorithm and heterogeneous multiscale methods. *SIAM Journal on Numerical Analysis*, 53(5):2472–2487, 2015. doi:[10.1137/140982374](https://doi.org/10.1137/140982374).

John Maclean and Georg A. Gottwald. On convergence of higher order schemes for the projective integration method for stiff ordinary differential equations. *Journal of Computational and Applied Mathematics*, 288:44–69, 2015. doi:<http://dx.doi.org/10.1016/j.cam.2015.04.004>.

Roland Maier and Daniel Peterseim. Explicit computational wave propagation in micro-heterogeneous media. *BIT Numerical Mathematics*, 59(2):443–462, June 2019. ISSN 1572-9125. doi:[10.1007/s10543-018-0735-8](https://doi.org/10.1007/s10543-018-0735-8).

Houman Owhadi. Bayesian numerical homogenization. *Multiscale Modeling & Simulation*, 13(3):812–828, 2015. doi:[10.1137/140974596](https://doi.org/10.1137/140974596). URL <http://dx.doi.org/10.1137/140974596>.

Daniel Peterseim. Numerical homogenization beyond scale separation and periodicity. Technical report, AMSI Winter School on Computational Modeling of Heterogeneous Media, <https://ws.amsi.org.au/wp-content/uploads/>

- [sites/70/2019/06/numhomamsi2019.pdf](#), 6 2019.
- R. Rico-Martinez, C. W. Gear, and Ioannis G. Kevrekidis. Coarse projective kmc integration: forward/reverse initial and boundary value problems. *Journal of Computational Physics*, 196(2):474–489, 2004. doi:[10.1016/j.jcp.2003.11.005](https://doi.org/10.1016/j.jcp.2003.11.005). URL <http://www.sciencedirect.com/science/article/B6WHY-4B8B9GY-1/2/e92e0d513d9f01c1a9c449d37d9d1a80>.
- A. J. Roberts. *Model emergent dynamics in complex systems*. SIAM, Philadelphia, jan 2015. ISBN 9781611973556. URL <http://bookstore.siam.org/mm20/>.
- A. J. Roberts and I. G. Kevrekidis. General tooth boundary conditions for equation free modelling. *SIAM J. Scientific Computing*, 29(4):1495–1510, 2007. doi:[10.1137/060654554](https://doi.org/10.1137/060654554).
- A. J. Roberts, Tony MacKenzie, and Judith E. Bunder. A dynamical systems approach to simulating macroscale spatial dynamics in multiple dimensions. *J. Engineering Mathematics*, 86(1):175–207, 2014. doi:[10.1007/s10665-013-9653-6](https://doi.org/10.1007/s10665-013-9653-6).
- A. J. Roberts, John Maclean, and J. E. Bunder. Equation-free function toolbox for matlab/octave. Technical report, [<https://github.com/ua1184615/EquationFreeGit>], 2020.
- Dirk Roose, Erik Nies, Ting Li, Christophe Vandekerckhove, Giovanni Samaey, and Yves Frederix. Lifting in equation-free methods for molecular dynamics simulations of dense fluids. *Discrete and Continuous Dynamical Systems—*

*Series B*, 11(4):855–874, April 2009. doi:[10.3934/dcdsb.2009.11.855](https://doi.org/10.3934/dcdsb.2009.11.855).

Saba Saeb, Paul Steinmann, and Ali Javili. Aspects of Computational Homogenization at Finite Deformations: A Unifying Review From Reuss' to Voigt's Bound. *Applied Mechanics Reviews*, 68(5), September 2016. ISSN 0003-6900. doi:[10.1115/1.4034024](https://doi.org/10.1115/1.4034024).

G. Samaey, A. J. Roberts, and I. G. Kevrekidis. Equation-free computation: an overview of patch dynamics. In Jacob Fish, editor, *Multiscale methods: bridging the scales in science and engineering*, chapter 8, pages 216–246. Oxford University Press, 2010. ISBN 978-0-19-923385-4.

S. Setayeshgar, C. W. Gear, H. G. Othmer, and I. G. Kevrekidis. Application of coarse integration to bacterial chemotaxis. *SIAM J. Mathematical Modeling and Simulation*, 4:307–327, 2005. <http://epubs.siam.org/sam-bin/dbq/article/60087>.

J. Sieber, C. Marschler, and J. Starke. Convergence of Equation-Free Methods in the Case of Finite Time Scale Separation with Application to Deterministic and Stochastic Systems. *SIAM Journal on Applied Dynamical Systems*, 17(4):2574–2614, January 2018. doi:[10.1137/17M1126084](https://doi.org/10.1137/17M1126084).

C. I. Siettos, M. D. Graham, and I. G. Kevrekidis. Coarse brownian dynamics for nematic liquid crystals: Bifurcation, projective integration, and control via stochastic simulation. *J. Chemical Physics*, 118(22):10149–10156, 2003. doi:[10.1063/1.1572456](https://doi.org/10.1063/1.1572456).